REPUBLIC OF AZERBAIJAN

On the rights of the manuscript

ABSTRACT

of the dissertation for the degree of Doctor of Philosophy

DEVELOPMENT OF A NEXT GENERATION NANOSATELLITE MODEL WITH LASER BEAM CONTROL AND ACTIVE TRANSPONDER SYSTEM

Specialty:	3325.01 – "Telecommunications technology"
Field of science:	Technical sciences
Applicant:	**Nadir Arzu oglu Atayev**

Baku – 2025

The work was performed at "Radio engineering and telecommunication" department of Azerbaijan Technical University.

Scientific Supervisor: Doctor of Technical Sciences, Professor
Mehman Huseyn oglu Hasanov

Official opponents: Corresponding Member of ANAS,
Doctor of Technical Sciences, Professor
Ali Mammad oglu Abbasov

Doctor of Technical Sciences, Professor
Anvar Tapdig oglu Hazarkhanov

Doctor of Technical Sciences, Professor
Bakhtiyar Magatil oglu Azizov

Dissertation council ED 2.41 of Supreme Attestation Commission under the President of the Republic of Azerbaijan operating at Azerbaijan Technical University.

Chairman of the
Dissertation Council: Doctor of Technical Sciences, Professor
Bayram Ganimat oglu Ibrahimov

Scientific Secretary of the
Dissertation Council: Doctor of Philosophy in Technical Sciences, Associate Professor
Zafar Alasgar oglu Ismayilov

Chairman of the
Scientific Seminar: Doctor of Technical Sciences, Professor
Famil Huseyn oglu Mammadov

GENERAL CHARACTERISTICS OF THE WORK

The urgency of the problem and degree of research. The implementation of inter-satellite link constellations in nanosatellites, particularly in low earth orbit, represents a significant advancement in this field. Optical communication systems offer substantial advantages over radio frequency communication in terms of high data transmission rates, low energy consumption, data security, and miniaturization potential. These benefits enable the resolution of challenges related to data transmission speed, frequency bandwidth, and security issues inherent in radio frequency.

The application of optical communication technology in nanosatellite inter-satellite link facilitates the rapid and reliable transmission of large volumes of data, supporting high-integrity real-time data exchange. From a technical perspective, the integration of laser beam sources, lightweight optics, and miniaturized steering mechanisms into the cubesat structure simplifies the incorporation of these components into nanosatellite platforms.

Key technologies in the application of optical communication systems include the Laser Ultra-miniaturized Encoder (LUME) by NASA, Commercial Off-The-Shelf (COTS) cubesat Laser Communication Terminals by MIT Lincoln Laboratory, the TeraByte InfraRed Delivery (TBIRD) system by MIT, the Laser Communication Demonstration (LCRD) by NASA, and the Space Optical Communications Research Advanced Technology (SOC-RAT) system by JAXA. The developers of these technologies have introduced new methodologies to achieve high speed and efficiency in optical communication. Collectively, these studies demonstrate that the implementation of optical communication technologies ensures the development of high-speed, reliable, and energy-efficient systems.

The theoretical relevance of this topic is underscored by critical parameters such as the saturation radiation index of the optical communication subsystem in the atmosphere, atmospheric attenuation coefficient, turbulence and attenuation indicators, output signal-to-noise ratio, pointing error indicator, ground station receiver aperture diameter, and inter-satellite link parameters. These factors can lead to atmospheric turbulence, optical radiation directionality, pointing errors, and other significant inaccuracies.

The practical significance of the dissertation topic lies in the design of a nanosatellite platform based on the preliminary engineering model of optical and radio frequency communication systems developed through these theoretical analyses. In this design, orbital analyses are conducted within the simulation tool kit (STK) environment, and the satellite's communication duration and the performance of the integrated optical communication systems are evaluated.

In conclusion, nanosatellites equipped with optical communication missions, especially in inter-satellite link topologies, play a crucial role in addressing communication challenges, ensuring high data transmission rates, and enhancing energy efficiency. They create conditions for achieving new results in inter-satellite communication and ensuring sustainable development.

Object and subject of research. The object of the research is the implementation of telecommunications systems on a nanosatellite platform. The subject of the research is the design and development of next-generation laser beam control and active transponder subsystems based on optical communication technology within the nanosatellite model.

Purpose and tasks of the work. The aim of the research is to develop a nanosatellite model focused on enhancing the technical performance, operational principles, and efficiency of next-generation laser beam control and active transponder subsystems.

The main tasks are as follows:

1. Designing and analyzing the effectiveness of nanosatellite platforms with "π ring-mesh topology" within satellite communication networks, based on orbital-mechanical parameters.
2. Analyzing the operating principles of optical and radio-

frequency communication networks for both space and ground segments and establishing a next-generation telecommunication network compatible with nanosatellite platforms.

3. Developing the architecture, software algorithms, and operating principles for optical laser communication, control and monitoring, and software-defined radio systems to be implemented on nanosatellite platforms.

4. Evaluating the impact of atmospheric turbulence on optical communication signals by analyzing quasi-dynamic and static indicators, and assessing their effects on the quality of communication channels.

5. Conducting preliminary engineering structural tests for cubesats based on theoretical calculations and STK simulation results on nanosatellite platforms and providing recommendations for their practical application.

Research methods. To achieve the objectives set forth in the dissertation, the study employs various methodologies, including principles of probability theory, system analysis theory, mathematical modeling techniques for atmospheric effects, theories of electrical communication, circuits, and measurements, quasi-dynamic and static modeling methods, numerical computation, computer modeling, and programming techniques.

Scientific statements submitted for defense:

1. Orbital-mechanical parameters of the "π ring-mesh topology" satellite communication scheme in low earth orbit, based on an initial engineering model of a cubesat, and methodologies for enhancing communication quality through the application of this topology.

2. Classification of existing optical and radio-frequency communication technologies in the context of nanosatellite platforms and methods for improving the efficiency of hybrid telecommunication systems through the combined use of both technologies.

3. Schematics of optical laser communication and command-control systems, microcontroller programming algorithms, and calculated performance metrics based on research and analyses

conducted within the cubesat structure.

4. Theoretical and practical modeling of the effects of atmospheric turbulence and quasi-dynamic and static atmospheric factors in optical laser communication systems, along with methods for improving the signal-to-noise ratio and the quality of the communication channel.

5. Methods for enhancing communication duration and technical performance metrics of nanosatellite platforms by simulating the satellite communication cluster cubesat architecture in an STK environment.

The scientific novelty of the research. The scientific innovations of the dissertation work are as follows:

1. The principle of constructing a hybrid telecommunication system through the integration of next-generation optical communication and radio-frequency communication technologies on a nanosatellite platform has been developed.

2. New functional block diagrams and algorithms have been proposed for the application of optical laser communication and command-control systems in the initial engineering model of a cubesat, supported by theoretical calculations.

3. Mathematical methods and models have been proposed for the probabilistic-temporal characteristics and atmospheric quasi-dynamic functions in optical communication theory, taking into account their application in cubesat structures with optical laser communication subsystems.

4. A mathematical model of the signal-to-noise ratio has been proposed, considering the effects of quasi-dynamic, static, and atmospheric turbulence factors on optical laser communication systems.

5. Based on the theoretical computational parameters and variables derived from the nanosatellite, a fully optical communication topology in the form of a "π ring-mesh structure" satellite communication cluster has been proposed for low earth orbit using the STK simulation and analysis environment.

Theoretical and practical significance of research. Based on the proposed initial engineering structure of the cubesat, various analytical and applied studies were conducted on the "π ring-mesh structure" satellite communication topology in low earth orbit, focusing on optical and radio-frequency communication ground segments. Within the scope of these studies, analyses of optical laser communication and command-control subsystems were performed, taking into account probabilistic-temporal characteristics and atmospheric quasi-dynamic parameters. Corresponding computational, simulation, design, and testing processes were carried out, resulting in the development of a physical model of a 4U cubesat.

Approbation and application of research. The main scientific, theoretical, and practical findings obtained in the dissertation have been presented and discussed at international and national conferences, symposia, and seminars, and have been published in relevant academic journals:

The 9th International Scientific-Technical Conference on "Informatics, Management, and Artificial Intelligence," Kharkiv, 2022; The 27th International Scientific Symposium "Let the Flag of the Turk Rise!", Baku, 2022; "Youth and Scientific Innovations" Scientific-Technical Conference at AzTU, Baku, 2022; The Republic Scientific-Technical Conference on "Energy Efficiency and Green Energy Technologies" at AzTU, Baku, 2022; The "International Conference on Engineering Sciences," Baku, 2022; The 5th International Conference on "Smart Communication Technologies and Virtual Mobile Networks," India, 2023; The 7th Scientific-Technical Conference on "Advanced Technologies and Innovations" at AzTU, Baku, 2023; The Scientific Conference "Space Technologies in Azerbaijan and the Genius of Heydar Aliyev" at MAKA, Baku, 2023; The "KANS 2023" International Scientific Seminar, Tehran, 2023; The 74th International Astronautical Congress (IAC), Baku, 2023; The 17th IEEE International Conference on Application of Information and Communication Technologies (AICT), Baku, 2023; The 5th International Conference on Problems of Cybernetics and Informatics (PCI), Baku, 2023; The 75th International Astronautical Congress (IAC), Milan, 2024.

Published works. 6 scientific articles and 15 conference papers reflecting the topic and findings of the dissertation have been published in national and international scientific-technical journals. Among these publications, 1 article has been published in the list of periodical scientific journals recommended for publication in the Republic of Azerbaijan, while 6 articles have been included in international abstracting and indexing systems of periodical scientific publications.

The organization in which the dissertation work was performed. The dissertation was conducted at Azerbaijan Technical University.

The total volume of the dissertation, indicating the volume of structural sections.

Dissertation work consists of introduction, Chapter III, 20 subsections. The volume of the introductory part of the dissertation is 8917, the volume of Chapter I is 34982, the volume of Chapter II is 35024, the volume of Chapter III is 46070 characters, the total volume is 127574 characters excluding the bibliography. The dissertation includes 82 figures, 18 tables, a 130-item bibliography and 3 appendices.

MAIN CONTENT OF THE STUDY

In the introduction the dissertation substantiates the relevance of the research topic, its scientific novelty, and practical significance. It defines the research objectives, analyzes new approaches and methods for addressing the research problems, and presents the main propositions submitted for defense. The scientific innovations, practical implications, scientific findings, as well as information on the structure, validation, and application of the research results, are all included in the work.

The first chapter provides a comprehensive analysis of the significance of the space environment and its impact on nanosatellite platforms, examining it in terms of its physical and dynamic mechanical parameters. The study focuses on the measurement parameters and structure of the space environment, its influence on satellite orbital motion, and critical factors essential for the operation of these platforms, such as orbital characteristics. The properties of low earth orbit and the atmospheric and mechanical effects experienced by these platforms are analyzed in detail using a flight-ready cubesat model.

In general, the historical development and phases of small satellite technology are thoroughly investigated, covering the substantial technical advancements and innovations in these satellite systems from their inception to the present day. These phases are enriched with detailed information about the subsystems of small satellites, the technologies employed, orbital operations, and mission outcomes. Additionally, the experiences gained, including the achievements and challenges encountered in various projects and missions, are specifically highlighted.

The operating principles of radio-frequency and optical communication systems used in telecommunications on nanosatellite platforms are analyzed comparatively, including satellite-to-satellite and ground-to-satellite communication structures, equipment, operational principles, and topologies.

Although existing radio frequency communication nanosatellite platforms are already being used at high performance levels, they remain a focal point of ongoing research in space. However, the use of continuously evolving optical communication technologies stands as one of the most critical challenges ahead. Based on a comparison of these two communication technologies, the following advantages of optical communication are highlighted [1]:

- High frequency bandwidth: Optical communication can transmit data at significantly higher speeds compared to radio frequency communication.
- Secure communication: Optical communication provides greater security against external interference with signals.
- Weight and compactness: Optical communication systems are smaller, lighter, and require less energy compared to radio frequency systems.

However, the limitations of optical communication have also been noted:

- Limited coverage: Optical communication requires a wide line of sight, making it challenging to ensure continuous connectivity in certain areas.
- Atmospheric effects: Optical communication signals can be adversely affected by atmospheric conditions such as fog and clouds.
- Precise beam alignment requirement: Maintaining precise beam alignment with moving satellites is more difficult to achieve.

Inter-satellite links are primarily established on radio communication and emerging free space optical network technologies, enabling direct data exchange between satellites and data transmission and processing in directions other than the ground station.

Based on certain parameters of the optical satellite network, the "π network" configuration has been selected, with recommendations to prioritize the following indicators:

- 6 orbital plane alignments (each at 30^0 intervals).
- 11 sets of satellites on each orbital plane line.
- Altitude around 500 km.
- Satellite tilt angle $\phi = 86.4^0$.

Based on the above, Figure 1 shows the conceptual visual diagram of the low earth orbit satellite cluster, its communication geometry and transmission line structure of the space and ground segments.

---

[1] Gibalina, Z., & Fadeev, V. Optical inter-satellite link in comparison with RF case in Cubesat system. – Russia, 2017. – 10 p.

Based on the principles of ring and toroidal satellite topology communication, it is possible to maintain (7/24) monitoring of any region using a single ground station. This is achieved by relaying data from one satellite, after it passes over the designated area, to another satellite within the same or a different orbital plane, as well as to the ground station. Alternatively, each satellite operates based on its specific orbit and movement trajectory over a designated region, providing extensive but short-duration communication coverage.

However, by leveraging the advantages of optical and radio-frequency communication, it is feasible to establish connectivity through a hybrid configuration with satellites within a selected orbital plane. This approach ensures high data volume and transmission speed, while minimizing latency, aligning with the superior characteristics of optical communication.

In Figure 1, the optical communication topology of cubesat satellites on an exemplary orbital plane, the wavelength index for intersatellite information exchange is represented by $\leftrightarrows \lambda_{1n,2n\ldots xn}$ while $\uparrow\downarrow \lambda_{1m,2m\ldots xm}$ denotes the wavelength index for mutual information exchange between the ground station and the satellite. Additionally, θ is the recorded divergence, in rad; ϕ is the tilt angle. d is the size of the receiving telescope, in meters and D *is* the aperture diameter of the optical beam, in meters respectively.

The proposed cubesat structure and its optical communication subsystem operate on the same principle as, the organization of communication functionality and the structural design of its components are analyzed in the following section.

Throughout the study, the cubesat structure was positioned in low earth orbit at an altitude of 500 km above earth's surface, with a potential data exchange distance of 2100 km. The initial data acquisition angle ratio was set at $\Phi = 10^0$, with the transceiver wavelength selected as $\lambda = 1550\ nm$.

This wavelength is particularly effective for optical communication systems, both spaceborne and terrestrial, due to its low attenuation coefficient. For full duplex communication with ground station, key parameters of the laser communication link were set as follows:

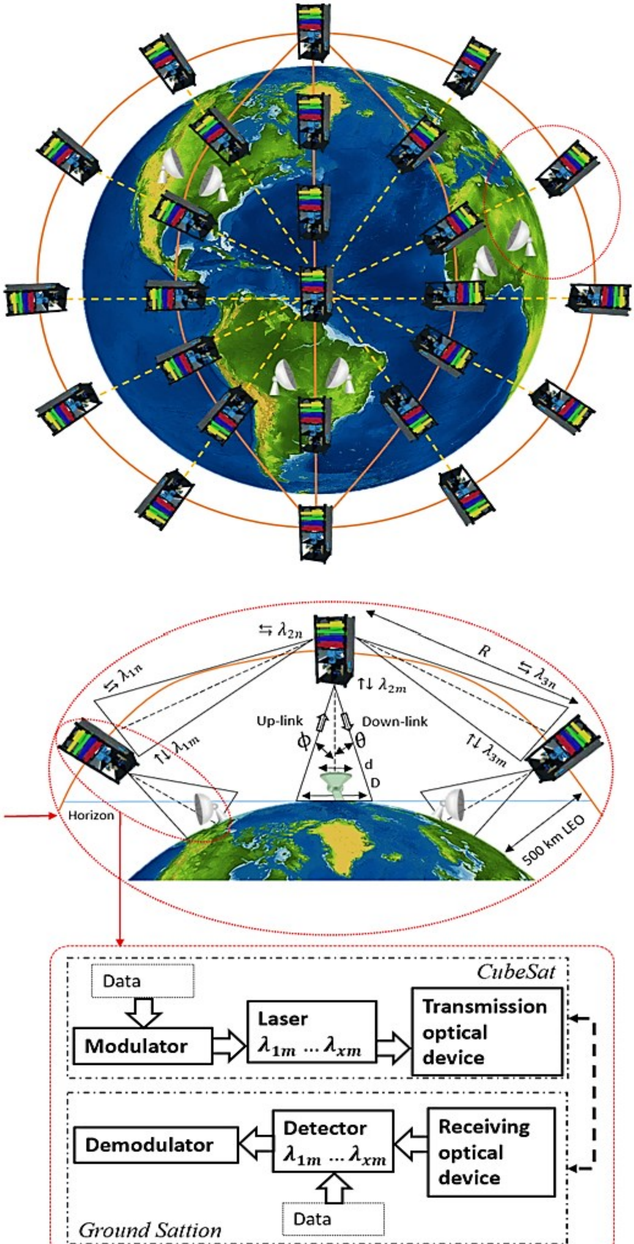

Figure 1. Proposed π ring-mesh low-earth orbit satellite communications array, its geometry and transmission diagram

the divergence angle $\theta = 100\ \mu rad$, the receiver telescope size $d = 60$sm, and transmitter power set at 1 W. Assuming that the sensitivity of the state-of-the-art receiver is approximately 1000 Ph/bit with a bit error rate of $1E^{-6}$, the required power level for data exchange with ground station and satellites in nearby orbits at a data rate of 10 Gb/s corresponds to -29 dB, as determined by the receiver's specifications.

Based on the analyses conducted, the optical communication controller and optical communication transponder subsystems employ laser diodes for data processing. This sets certain requirements for the optical communication systems, including the need for the beam source and carrier medium to align with one of the transparency windows of the optical fiber. The output beam power must be sufficiently high, and its insertion into the optical medium must be efficient. Additionally, the optical beam should support various modulation methods, with requirements for minimal power consumption, compact size, and lightweight characteristics.

In the second chapter the initial stages of the satellite production phase are discussed, with a focus on the cubesat preliminary engineering model. Before designing and preparing the this model, the significant results achieved thus far are compiled in Table 1. These results serve as the foundation for developing the flight ready model, which acts as the baseline for the selection or design of nearly all necessary subsystems in subsequent studies.

The design of the optical communication subsystem with control and transponder units can be implemented in stages, starting with the development of the functional block diagram of the subsystem, followed by a three-phase design process and the detailed development of each individual component. Figure 2 illustrates the functional block diagram of the 3U cubesat's general optical communication subsystem. The diagram depicts two main bus channels: the first is the data bus, which integrates all input-output interfaces and ports, and the second is the power bus, which supplies the necessary electrical power to all subsystem components.

Table 1
Performance metrics calculated prior to cubesat preliminary engineering model design

Given/parameter	Value/indicator
Inter satellite network topology	π array of satellites on orbital plane with 6 orbital plane alignments (each at 30^0 interval) in a ring-grid structure
Satellite and orbital plane tilt angle/Eccentricity (ϕ)	86.4^{0}
The orbit or semi-major axis (a)	$6.878 * 10^3$ km
Orbit altitude and position (H_{orbit})	Low earth orbit 500 km circular orientation
Period of complete rotation in orbit (T_{orbit})	1.57 hours $= 94.2$ min ≈ 95 min
Velocity of the orbit and the satellite with it (v_{orbit})	7.61 km/sec
Earth surface dark period (T_{dark})	0.58 hours $= 34.8$ min
Lifetime of earth's surface (T_{light})	1.17 hours $= 70.2$ min
Optical communication subsystem wavelength (λ_{OR})	500 nm $- 2000$ nm
Root-mean-square wavelength ($\sqrt{\lambda}$)	1250 nm
Cubesat 2U structural mass (m)	3 kg
Output power of the optical laser beam transmitter (P_{TX})	1 W
Aperture diameter of receiver diaphragm (d)	0.1 m
Plane optical beam diameter (D)	10 km
Radial divergence (θ)	0.001 radians

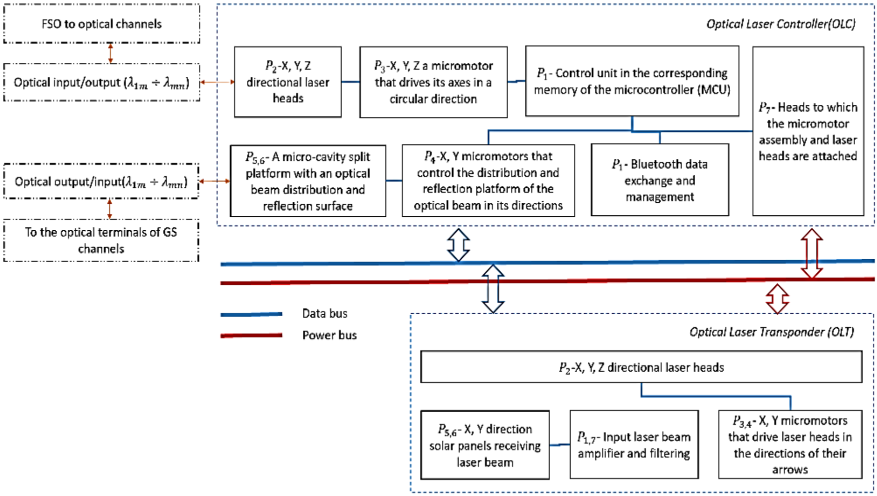

Figure 2. Functional diagram of the parts comprising the cubesat 2U optical laser communication system

As shown, the diagram is divided into two sections: the optical communication control subsystem and the transponder subsystem. The design and functionality of each are described in detail below.

Regarding the operational logic of the designed subsystem, signals from the control block are transmitted as pulse-width modulation signals to the laser head and semi-transparent mirror servo micromotors, ensuring their rotation to the required angle. Additionally, via another digital output interface, the activation of each laser is carried out based on incoming commands. Consequently, the laser beam directed at the semi-transparent layer is reflected in four directions through servo system movements.

The operational principle of the designed optical communication transponder subsystem is as follows: the Mega2560 microcontroller drives the servo micromotors with a rotation angle range of 0^0-180^0, simulating orientation along the X, Y, and Z axes. This also ensures the angular alignment of the ground station's solar panels with the incident beam ϕ, thereby enabling three-dimensional spatial movement. This process, along with detailed information on the internal components and key functionalities of the 3U optical communication structure, is further elaborated in subsequent subsections.

For the design of the radio-based control and monitoring system, the main communication subsystem integrated into the 1U structural configuration was equipped with a radio-frequency module for desktop testing and long-distance radio communication, supported by ground-based software. The schematic of this structure is presented in Figure 3.

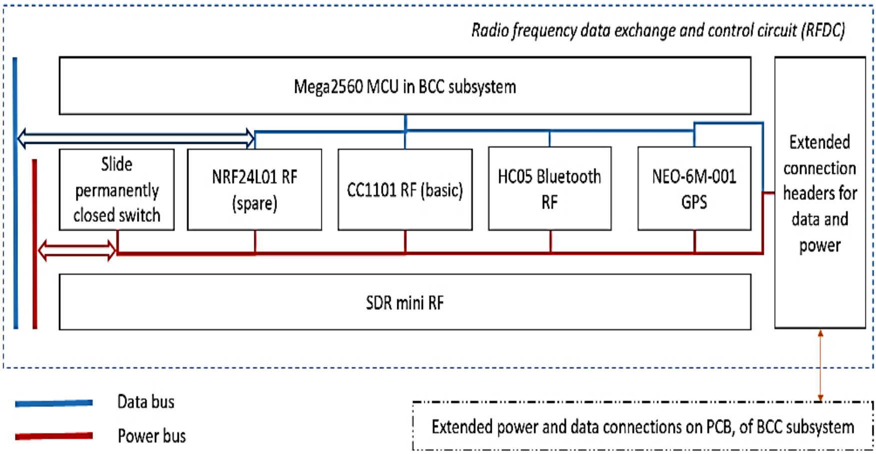

Figure 3. Functional block diagram of a cubesat radio communication circuit

As illustrated in the Figure above, all components of the circuit begin functioning once the main input switch is activated, allowing electrical power to flow from the power circuit subsystem. The onboard computer circuit subsystem processes and aggregates data, which is then transmitted to the ground station via the CC1101 radio-frequency transmitter module. The NRF24L01 radio-frequency module serves as a backup for the primary radio-frequency communication module and is primarily utilized for closer distances or communication with alternate ground stations in the event of data transmission interruptions. The NEO-6M-001 module is designed to determine the platform's geographical orientation and serves as a crucial part of the positioning and control subsystem.

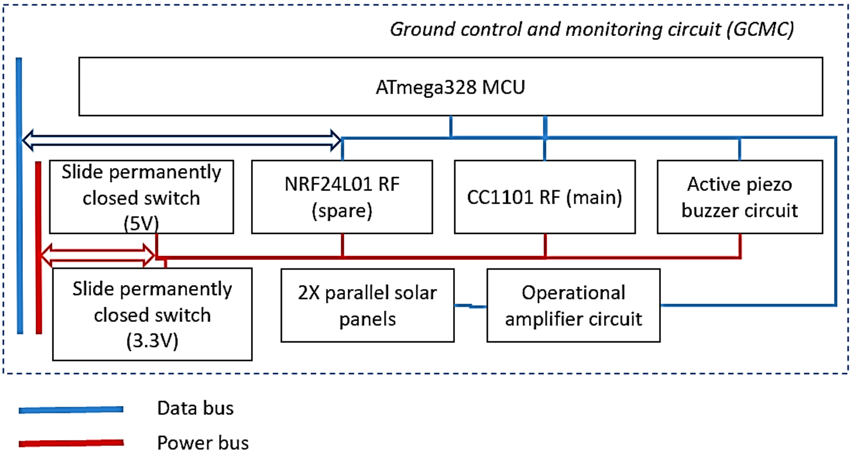

Figure 4. Functional block diagram of a cubesat ground station circuit

As shown in Figure 4, the Atmega328 microcontroller is connected to 5 V and 3.3 V voltage sources, ensuring the power supply to all components and modules. Simultaneously, a unified optical communication beam of binary 0 and 1 levels, received via two parallel-connected solar panels, is initially amplified through a non-inverting operational amplifier circuit and then connected to the analog terminal of the microcontroller for processing. During this process, the system remains in constant communication with the user interface. Similar to the radio communication circuit, the CC1101 radio-frequency module is employed here for primary radio data exchange. Additionally, an active piezo buzzer is connected to the microcontroller's digital terminal, providing audible alerts for critical information.

In this research, a structural analysis of program algorithms for the onboard computer and positioning and control subsystem interface circuits has been conducted. The Atmega328 microcontroller was employed as the main data management component in the ground station circuit. A specialized software environment was developed to facilitate data exchange and signal processing between external interface modules and components within the microcontroller-based system. For this purpose, the structural functions of the cubesat's initial engineering model were pre-programmed in C++ and loaded into the microcontroller's cache memory.

As noted, the processing of sensor and module data within this circuit not only ensures the cubesat's positioning and control functionality but also plays a critical role in managing and sharing data across the optical laser communication system, the radio data circuit, and the electrical power subsystem. The functional block diagram of the onboard computer circuit, designed for this purpose, is presented in Figure 5.

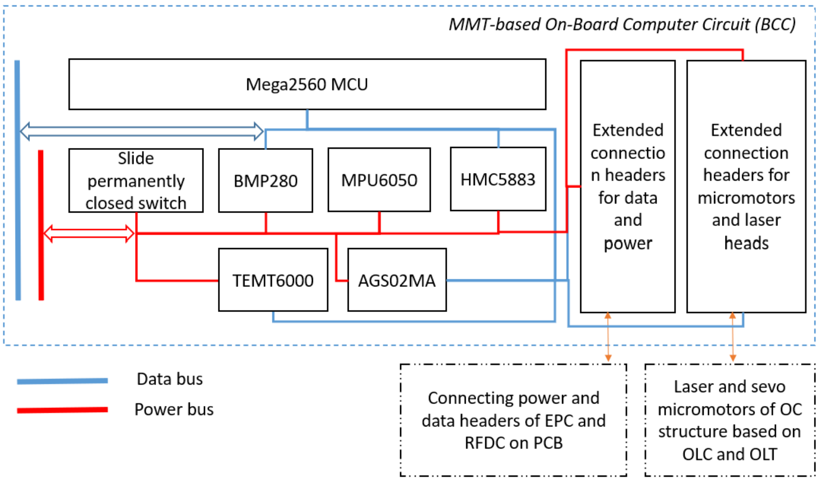

Figure 5. Functional block diagram of the cubesat onboard computer circuit subsystem

As illustrated in Figure 5, the unregulated 8.4 V Li-ion battery pack supplies voltage to the input of the Mega2560 microcontroller. This voltage is then distributed to the power terminals of all circuit components through the internal 3.3 V and 5 V linear regulators. The circuit incorporates interfaces for optical laser communication subsystems specifically, the optical communication control and transponder servo micromotors, laser heads, as well as connectors to integrate the power circuit and radio communication subsystems' respective data and power lines.

In designing the cubesat's initial engineering model structure, one of the primary functions of the control- and monitoring-based power circuit subsystem is to supply electrical energy to all subsystems. The proposed engineering model structure includes a power subsystem designed with redundancy in its components to ensure reliable energy generation and autonomous power supply. The functional block diagram of this subsystem is depicted in Figure 6.

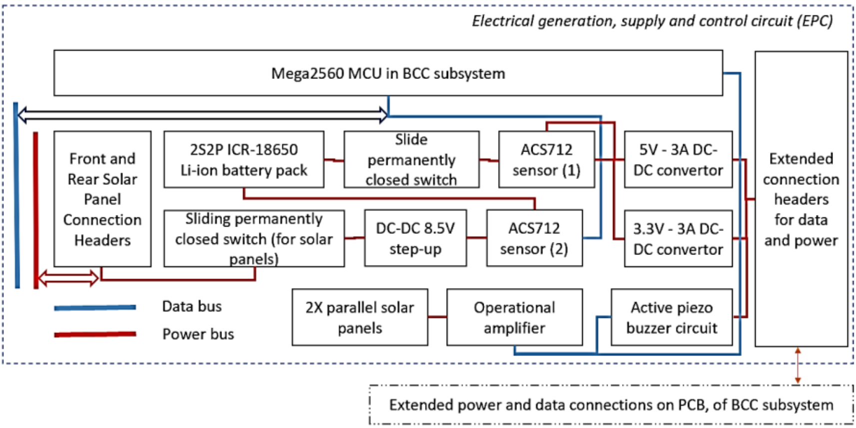

Figure 6. Functional block diagram of the cubesat power supply circuit subsystem

Upon analyzing the operating principles of the circuit shown in Figure 6, it was determined that the approximately 5.5 V, 170 mA electrical output from the solar panels is insufficient to fully charge the 2S2P 18650 Li-ion battery pack, which provides continuous power to the platform. To address this, a voltage booster circuit is employed to raise the voltage to 8.5 V, which is then directed to the input of the ACS712 current and voltage sensing module. Simultaneously, energy drawn from the batteries passes through another ACS712 sensor via an electrical switch and is delivered to

5 V-3 A and 3.3 V-3 A constant-current converters.

Due to space constraints on the onboard computer circuit managing the optical communication transponder subsystem, certain functionalities such as the operational amplifier for the solar-panel-based optical beam receiver and the parallel sound-indication active buzzer circuits are executed sequentially in accordance with the optical communication program algorithm.

In the third chapter, the optical communication and radio frequency communication network subsystems, along with their functionalities and roles in executing telecommunications-based missions, are extensively analyzed. The operational principles, functional capabilities, and application domains of these subsystems are thoroughly investigated. Additionally, the efficiency of optical communication and radio frequency network subsystems is discussed in detail, focusing on their compatibility with nanosatellite platforms and identifying potential application areas.

In recent years, the adoption of software-defined radio platforms has gained significant attention. The primary advantages of these platforms include low power requirements (1 W–10 W), wide frequency ranges (50 MHz–8 GHz), broad frequency sampling bandwidths (32 MHz–56 MHz), and, most importantly, the ability to control traditional radio frequency communication components (e.g., mixers, modems, codecs, filters, etc.) through field-programmable gate arrays (FPGAs)[2]. These features provide extensive opportunities for integration into cubesat structures, enabling the seamless operation of radio frequency and optical communication systems, automatic adaptation to required frequency bands in radio frequency communication-based mobile ground stations, and efficient retransmission of weak signals.

The optical communication control subsystem, as one of the most critical subsystems of the cubesat structure, represents a new application direction derived from previous scientific and practical research (e.g., next-generation 3D optical switches). The current

[2] Joshi, M. P., Patil, S. A., & Shimpi, D. C. Design and implementation of BPSK audio transmitter & receiver using SDR. – India, 2017. – 5 p.

system ensures the operational routing of optical switches, the architectural optimization of optical networks, and the effective use of optical fiber transmission systems in localized settings. It enhances the speed and efficiency of information flow and communication switching while offering the following advantages:

- The ability to utilize laser light sources in a compact, 360^0 rotating assembly of lenses, reducing size, material usage, and overall cost.
- Control of the laser heads via high-precision microactuators, which improves switching time and signal direction when using semi-transparent mirrors.
- Continuous monitoring and diagnostic capabilities through an integrated electronic control and measurement system.

The optical communication transponder subsystem, unlike active radio frequency transponders, enables optical communication with the ground station through full-duplex transmission using a three-axis (x, y, z) laser-head emitter and photodetector receiver. This subsystem provides an advanced communication link for the cubesat structure. During the design phase of the cubesat flight rady model, environmental and structural interactions were analyzed through mathematical modeling, and mission parameters were initially tested in a computer simulation environment. The variation in the intensity (σ_R^2), which directly depends on the scale of atmospheric turbulence, was analyzed on the cubesat preliminary model in MATLAB[3].

$$\sigma_R^2 = 1.23 C_n^2 k^{\frac{7}{6}} z^{\frac{11}{6}} \tag{1}$$

Where C_n^2 represents the optical refractive index structure parameter associated with atmospheric turbulence, in $m^{-\frac{2}{3}}$; $k = 2\frac{2\pi}{\lambda}$

[3] Maharjan, N., Devkota, N., & Kim, B. W. Atmospheric effects on satellite–ground free space uplink and downlink optical transmissions. // Appl. Sci., 2022, 12, – p. 10944.

is the optical wave number, in m^{-1}; z denotes the link distance (500–2000 km), in meters.

The resulting mathematical curve is shown in Figure 7. Channel time variation is calculated using a theoretical quasi-static model, commonly referred to as the frozen (or stopped) channel model. This model assumes that the channel fading remains constant throughout a symbol frame (coherence time) and changes to a new value between successive frames.

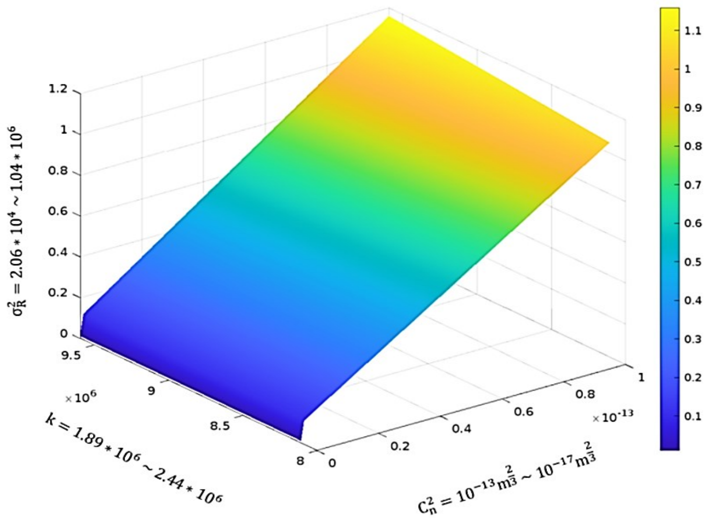

Figure 7. Dependence of the output optical beam turbulence on the dispersion intensity

From the resulting curves, it can be observed that the space atmospheric environmental effects, expressed as $\exp \uparrow (\sigma_R^2, C_n^2)$, directly contribute to a deviation in the value across both axis planes. This deviation can be attributed to dynamic adjustments in the reflectivity and directivity of the 3D optical switch, which are designed to ensure maximum line-of-sight transmission (D) and minimize the effects of turbulence on the optical communication system.

The saturation radiation index through the atmosphere in low earth orbit, similarly influenced by atmospheric turbulence, was analyzed in MATLAB, with the resulting mathematical curve presented in Figure 10:

$$I_{full} = \frac{0.37(n-1)^2 P}{(2r^2)e^{\left(-\frac{2.77}{h}\right)}} \text{ ,} W/m^2 \tag{2}$$

Where n is the refractive index of the atmosphere; P denotes the power of the optical signal, in watts; r is the radius of the receiver aperture, in meters; and h is the height of the receiver.

To make the appropriate calculation, refer to Table 1 is low earth orbit H height, optical transmitter output power P_{TX} , and λ_n output wavelength range.

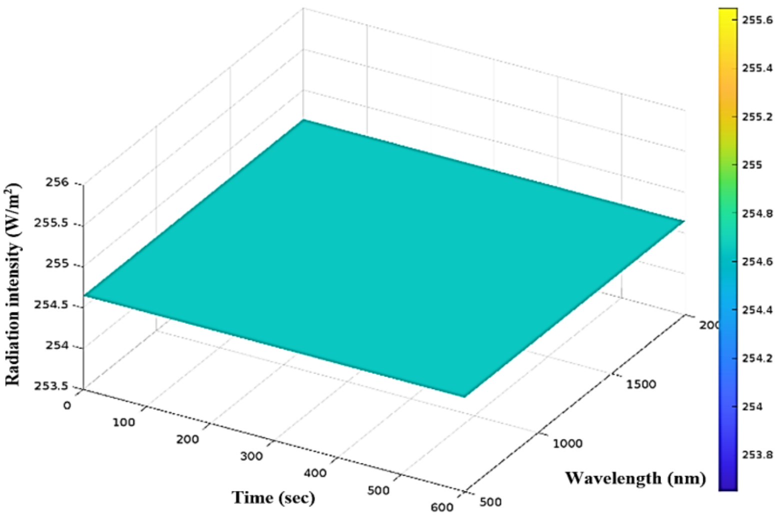

Figure 8. Atmospheric attenuation of saturational radiation in low earth orbit by time and wavelength

Based on the characteristics of the obtained curve, it can be noted that the intensity of saturation radiation primarily exhibits a linear proportionality dependent on the wavelength variation.

The impact of turbulent atmospheric conditions on FSO optical signals was evaluated for wavelengths of $\lambda = 1.31\, mkm, \lambda =$

$1.55\ mkm, \lambda = 1.62\ mkm$. The dependency graph on the signal-to-noise ratio is presented in Figure 9.

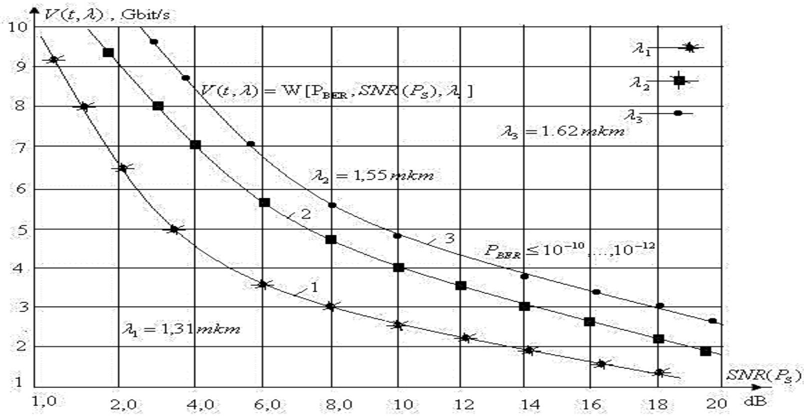

Figure 9. Dependence of the transmission rate on the signal-to-noise ratio in optical spectrum-division multiplexing channels of free space optics

As shown in Figure 9, the use of spectral compression systems in free-space optics leads to an increase in the number of optical channels, thereby enhancing the system's transmission capacity by $C_{max}(\Delta F_k, \lambda_i, N_k)$.

Regarding the impact of atmospheric conditions on the quality parameters of optical signals, the approximate relationship between transmitter and receiver terminals for satellite-to-satellite, satellite-to-ground, and ground-to-satellite links is analyzed in terms of signal-to-noise ratio (SNR), a key metric for evaluating the performance of optical systems[4].

$$P_{transmitter} = P_{receiver} \frac{d_L^2}{(d_T + \theta L)^2} 10^{-\alpha \frac{L}{10}}, W \quad (3)$$

Where $P_{transmitter}$ represents the transmitter power, in watts; d_L is the diameter of the receiver aperture; d_T is the diameter of the

[4] Chan, W. S. Free-space optical communications. // J. Lightwave Tech., 2006, 24(12), – pp. 4750-4762.

transmitter aperture, in meters; θ is the divergence angle, in radians; L is the distance between the transmitter and receiver; and α is the atmospheric attenuation coefficient, in dB/km.

It is well known that atmospheric inhomogeneities, along with variations in temperature and air pressure, influence the intensity of light scintillation and the medium's thermal coefficient, leading to optical turbulence. Various models have been developed to describe the intensity fluctuations of optical scintillation. These channel models simulate a wide range of gamma turbulence, with the probability density function defined as follows[5]:

$$P(I) = \frac{2(\alpha\beta)^{\frac{\alpha+\beta}{2}}}{\Gamma(\alpha)\Gamma(\beta)} I^{\frac{\alpha+\beta}{2}-1^{-1}} K_{\alpha-\beta}(2\sqrt{\alpha\beta I}) \quad (4)$$

Where $\alpha\beta$ are the parameters of the statistical distribution; I denotes light intensity, in W/m^2; $\Gamma(x)$ represents the gamma function; and $K_{\alpha-\beta}$ is the modified Bessel function of the second kind.

In general, the SNR, a widely used indicator of communication channel quality, is defined as:

$$SNR(P_S) = Q_F \cdot \frac{\Delta F_E}{\Delta F_k} [(1+r)/(1\text{-}r^{0.5})^2] \quad (5)$$

Where Q_F is the quality factor; ΔF_E is the effective frequency bandwidth, in Hz; ΔF_k is the channel bandwidth, in Hz; and r is the reflectivity coefficient.

The analysis of atmospheric turbulence effects on the pointing error indicator of optical communication subsystems shows that it influences not only the signal-to-noise parameter but also the GS pointing accuracy for optical radiation.

---

[5] Carrasco-Casado, A., & Mata-Calvo, R. Free-space optical links for space communication networks. – Japan, 2020. – 66 p.

This dependency manifests as pointing and directional errors and is expressed by the following relation. Similar to saturation radiation and turbulence throughout the atmosphere, the cubesat preliminary engineering model's pointing error indicator was analyzed in MathLab, and the results are presented in Figure 10.

$$\Delta\theta = \left(1.22\frac{\lambda}{d*\phi}\right) * (k^2L^2C^2)^{\frac{3}{5}} * \int_0^L \left(\frac{z^{\frac{5}{3}}}{L}\right)dz \qquad (6)$$

Where λ represents the wavelength of the optical signal, in meters; d is the diameter of the receiver aperture. Other parameters are as defined in the intensity expression.

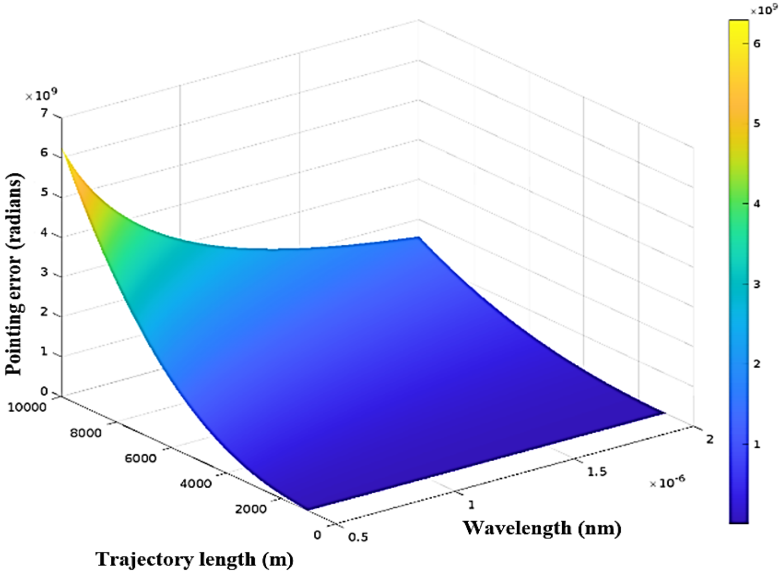

Figure 10. Directional error indicator based on wavelength values of selected low earth orbit heights

Finally, aerosol and cloud models, which impact optical signal attenuation in the atmospheric environment, were considered. Fog and rain cause significant scattering and absorption of optical signals, and light scattering reduces the reliability of communication links.

Analyzing these attenuations is essential for the robust design of free space optic communication systems, making it invaluable in enhancing the performance and reliability of optical communication.

Considering a root-mean-square wavelength of $\lambda = 1250\ nm$, visibility of 10 km, and a qualification constant of $q = 1.3$,

$$\alpha_{visibility} = \left(\frac{3.91}{visibility}\right)\left(\frac{\lambda * 10^9}{550}\right)^{-q} = 0.4\left(\frac{1250}{550}\right)^{-1.3} \approx 0.12, dB/km \quad (7)$$

After MATLAB calculations, the graph presented in Figure 11 illustrates the dependency of fog and rain attenuation on optical wavelength. According to this graph, attenuation starts at approximately 0.45 dB/km at 500 nm and decreases to 0.05 dB/km at 2000 nm. Fog attenuation remains stable at around 0.15 dB/km, while rain attenuation reaches a value of 0.05 dB/km.

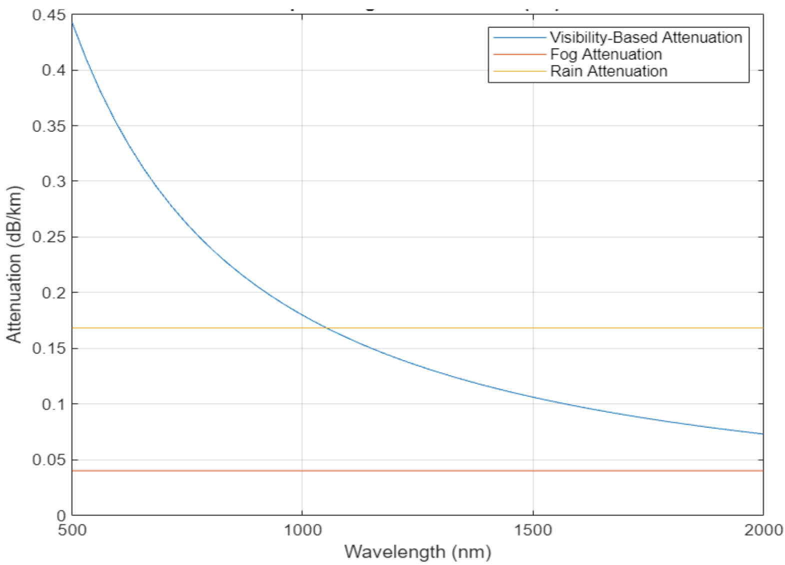

Figure 11. General dependence of the optical signal on the meeting zone from fog, rain-based attenuation

Aerosol and cloud models, including aerosol distribution models, Mie scattering, cloud cover effects, and liquid water content, provide a detailed description of the impact of particles on optical signal attenuation. Mie scattering analyzes how particles scatter light, thereby affecting signal clarity.

Considering a root-mean-square wavelength of $\lambda = 1250\ nm$, with a particle density of $N = 10 * 10^6 \frac{particle}{m^3}$ and a scattering index of $m = 1.5$,

$$\sigma_{scattering} = Q_{scattering}\pi a^2 = \left(\frac{2m^2}{m^2+2}\right) x^2 \pi a^2 = 3.34 * \pi * (0.5 * 10^{-6})^2 \approx 2.62 * 10^{-12} \quad (8)$$

When calculating aerosol attenuation, N represents the aerosol concentration,

$$\alpha_{aerosol} = N\sigma_{scattering} \approx 2.62 * 10^{-5}\ dB/km \quad (9)$$

Where $Q_{scattering}$ is the scattering coefficient; m is the refractive index; and a is the radius of the particle,

$f_{cloud} = 0.5, \gamma_{cloud} = 0.2\frac{db}{km}\ in\ every\ \frac{g}{m^3}, LWC = 0.3\frac{g}{m^3}$ cloud attenuation can be defined as,

$$\alpha_{cloud} = f_{cloud}\gamma_{cloud}LWC = 0.03\ dB/km \quad (10)$$

Where f_{cloud} is the cloud coverage fraction; γ_{cloud} represents the attenuation coefficient, taken as 0.2 dB/km for every q/m^3.

Figure 12 illustrates the attenuation of optical signals due to cloud cover as a function of cloud cover fraction and wavelength. When cloud cover is complete (fraction 1), attenuation is approximately 0.2 dB/km at 500 nm and decreases to about 0.05 dB/km at 2000 nm. For lower cloud cover fractions (0.2–0.6), attenuation varies between 0.02 dB/km and 0.1 dB/km across the wavelength spectrum, showing a significant reduction.

Figure 13 illustrates the Mie scattering efficiency as a function of aerosol radius and wavelength. When the aerosol radius is 10^{-6} meters, the scattering efficiency reaches its peak value of 180 and then sharply decreases as the wavelength increases. When the aerosol radius exceeds $0{,}4 \times 10^{-6}$ meters, the scattering efficiency drops below 50 across all wavelengths.

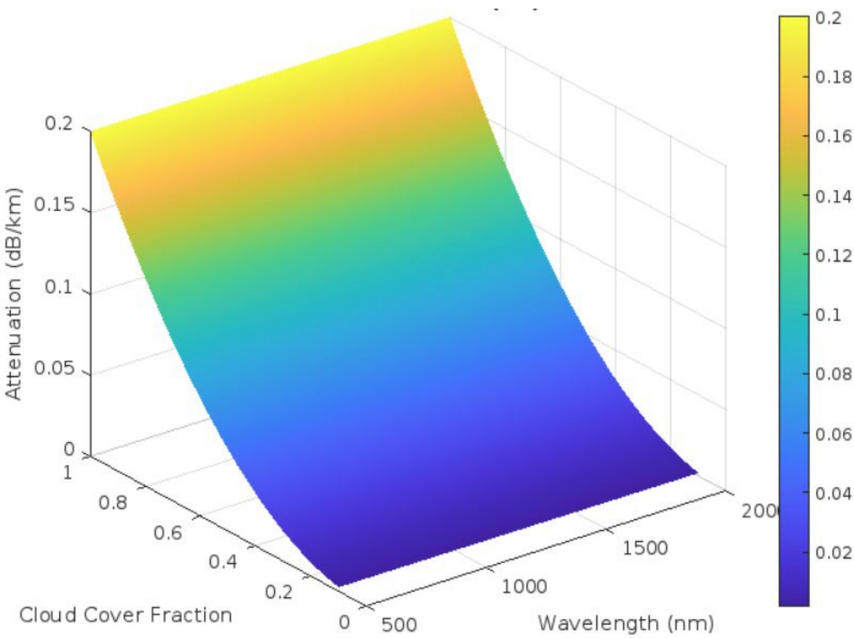

Figure 12. Dependence of cloud attenuation on rms wavelength range

Based on the obtained curves, it can be stated that the pointing error is directly dependent on the selected wavelength parameter and exhibits multiple values due to stochastic inverse exponential variation.

In this study, since the orbital and initial structural parameters of the 2U cubesat attitude determination and control system is known, the first scenario was analyzed within the STK environment:

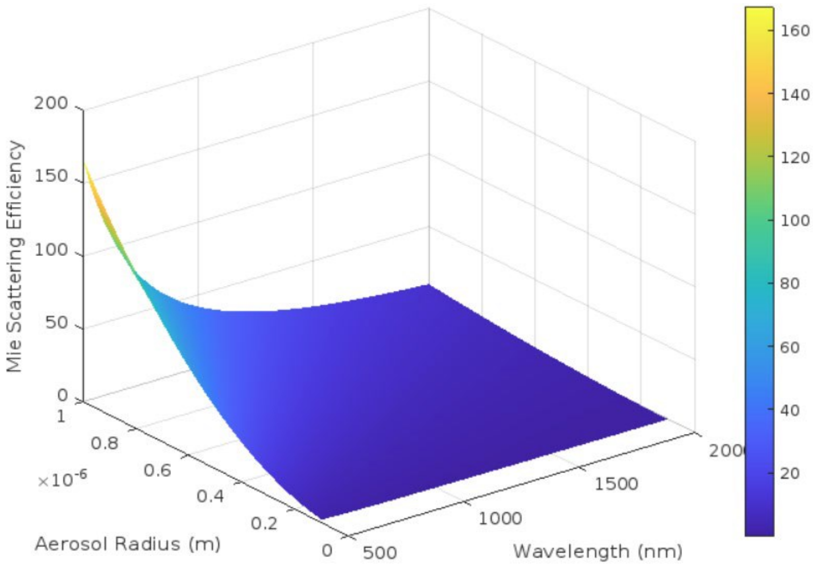

Figure 13. Dependence of the Mie scattering efficiency on the rms wavelength range

• An ISL π-ring-grid-based simple orbital planar array of satellites.

• An analysis of OLC irradiated satellite clusters with a planar structure in the same orbit.

The design and analysis steps for the first case can be outlined as follows:

• A new mission window is created, as detailed in Table 2, where important data such as H, ϕ, and t are entered.

• In the selected orbit, the new 2U cubesat model and its predecessors are assigned critical parameters including m, A, C_q, etc. Additionally, the surface friction area with respect to the ground ($\rho_Y = 0.029$) and the surface friction area with respect to solar radiation ($\rho_G = 0.064$) are established as the two primary indicators for the satellite. Initially, a maximum operational duration of 10 years is simulated to determine their values.

• Finally, based on the integrated atmospheric and solar density indicators within the program environment, the average values of the key results obtained for the cubesat's on-orbit/survival time are presented in Table 2.

Table 2

Analysis results from the 2U flight ready model cubesat mission in the STK simulation environment

Eccentricity	Height of perigee	Height of apogee	Orbital period	Number of orbital revolutions	Satellite lifetime
86.38^0	434.4 km	450.43 km	1.55 hours	21,613	3.8 years

Upon reviewing the results in Table 2, it is observed that the eccentric orientation angle transitions from 86.4° to 86.38°, while the altitudes of apogee and perigee are recorded within a range of 500 km to 450 km. The orbital period is calculated and approximated to 1.75 hours and 1.55 hours, as determined in the previous section.
Consequently, each satellite within the inter-satellite link at low earth orbit exhibits an operational lifespan of 3.8 years, equivalent to 21,613 complete orbital cycles.

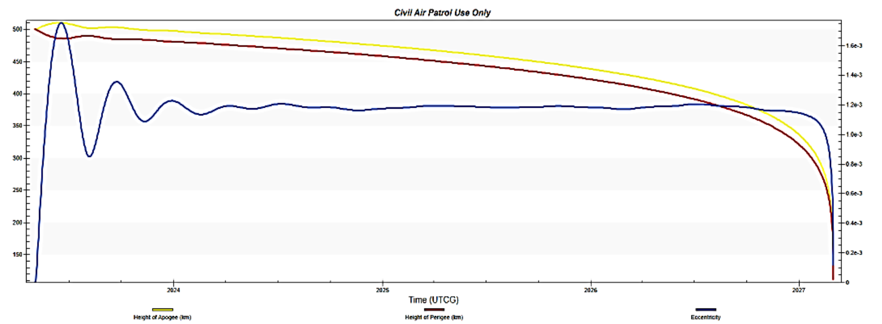

Figure 14. Lifetime of 2U cubesat flight ready model in orbit during 2024-2027

Analyzing Figure 14 reveals that the satellite's eccentricity initially peaks at around 400 km as it is launched into orbit from earth's surface. With the spiral motion controlled by the inertial and altitude management subsystem, it reaches 500 km and then stabilizes at approximately 350 km from 2024 through 2027.

In subsequent steps, as analyzed in the first and second cases concerning the satellite constellation in low earth orbit:

- Based on the flight-ready parameters of the initially developed 2U cubesat model, six orbital planes with a π-ring-mesh structure were generated in different meridian directions, as outlined in Table 2. Each orbital plane was designed with radial separations of 30° and populated with 11 nanosatellites, named accordingly from cubesat101 to cubesat611. A 3D spatial representation of this configuration is depicted in Figure 15.
- As an example, Figure 16 illustrates the visual output in the STK environment after alignment with the structural specifications of the designated flight-ready model. This visualization demonstrates the satellite's unidirectional movement along the precise northern axis, as well as its positioning to enable the corresponding movement of optical communication control and transponder subsystems.
- Additionally, the final step in the STK environment involved ensuring complete optical communication in nadir, zenith, north, and south directions. This was achieved by configuring the optical communication control and transponder subsystems to align along the meridians and parallels of the same orbital plane, with visualizations provided for the optical communication beams in four axes for each satellite.

Based on all simulations conducted in the STK environment and the satisfactory results obtained, the development of the 2U cubesat flight-ready model facilitated the establishment of an infrastructure for reciprocal and complete optical laser communication between nanosatellites and between nanosatellites and ground stations.

As a result, an engineering prototype of a 4U cubesat structure equipped with a next-generation laser beam controller and active transponder system was developed and tested, as shown in Figure 17.

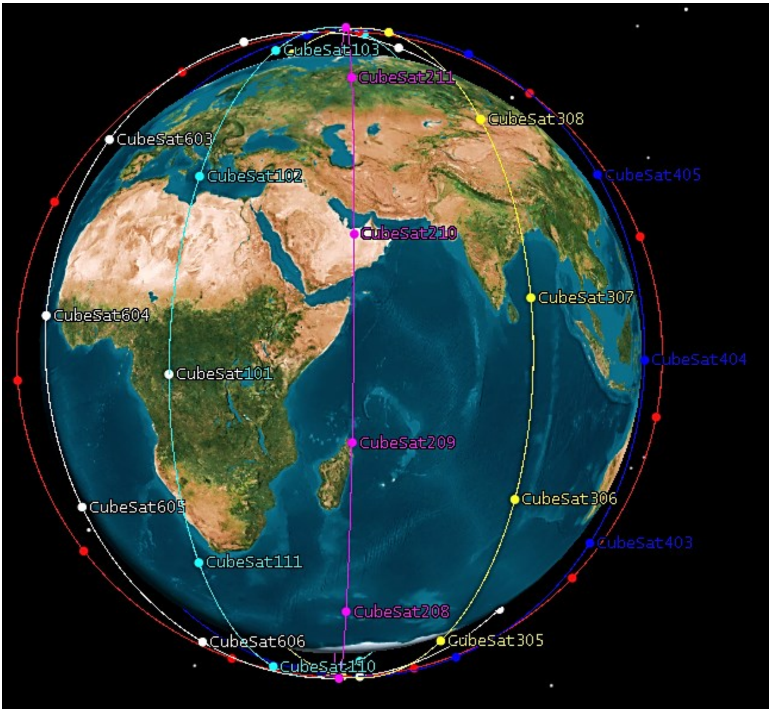

Figure 15. π 3-dimensional model of a ring-mesh low-earth orbit satellite communications constellation in a STK environment

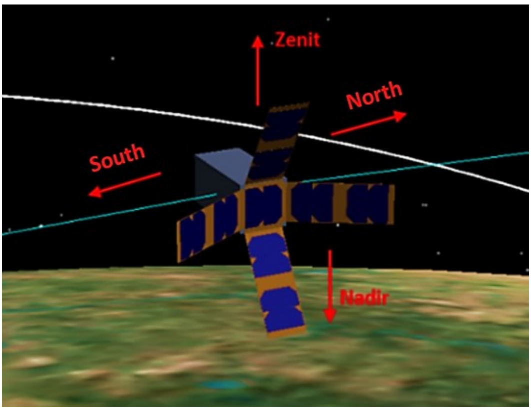

Figure 16. Orbital positioning and orientation of the 2U cubesat flight model

Figure 17. A completed real-world view of the 4U cubesat preliminary engineering model structure

Figure 18 showcases the ground station system's connection to a user computer via a USB interface. The user interface of the software, which facilitates autonomous communication between the cubesat structure's radio-frequency and optical laser communication subsystems and ensures mutual data exchange, is displayed.

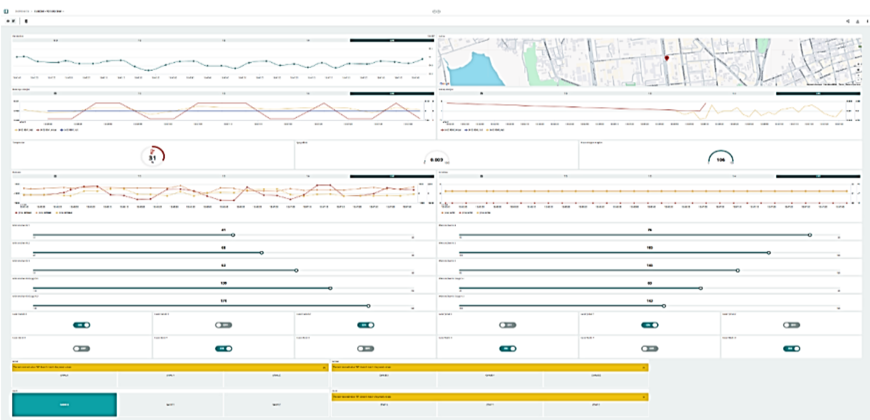

Figure 18. Interface of the control and monitoring structure software for the ground station user

CONCLUSIONS

1. For the first time, the construction of nanosatellite platforms based on the "π ring-mesh topology" satellite network has been proposed. The system consists of 66 satellites organized into 6 orbital planes, each spaced 30° apart, with 11 nanosatellites per plane. The placement of nanosatellites at an altitude of 500 km ensures minimal latency in optical communication. The orbital plane inclination was chosen as $\varphi = 86.4°$, and the satellite orbital period is $T = 90$ minutes [8,13].

2. In the proposed π topology, inter-satellite data exchange is established via optical communication at wavelengths λ_{1n}, λ_{2n} … λ_{xn}, while communication with ground stations is achieved using wavelengths λ_{1m}, λ_{2m} … λ_{xm}. Beam divergence was calculated using the formula $\theta = 1.22\ (\lambda / D)$, and latency was maintained within a range of 5 µs/km. Compared to radio frequency systems, transmitters with 1 W power and receivers with a sensitivity of -65 dBm were used [2,4].

3. Optical communication technology demonstrated a data transmission rate of 2.5 Gb/s, smaller antennas (10.2 cm), lower power consumption (93.8 W), and lightweight transponders (65.3 kg). These metrics outperform radio frequency technology, which requires larger antennas (2.2 m), higher power consumption (213.9 W), and heavier transponders (152.8 kg) [1,3,5].

4. It was shown that optical communication in nanosatellites at a wavelength of 1550 nm or frequency of 193 THz is optimal for reducing atmospheric attenuation and achieving a data transmission capacity of 10 Gb/s. Optical communication technology offers a viable alternative to radio frequency systems in terms of antenna size, power consumption, and mass [9].

5. Optical laser systems support full-duplex communication over distances of 500–2000 km. Their narrow, coherent, and highly efficient beams reduce energy consumption. In a hexagonal packing model, 33% fewer points were required [20].

6. Advanced architectures employed laser diodes and servo micromotors. The optical communication module achieved a

transmission rate of 1 Mbps with an effective range of 5–10 km. Software-defined radio architectures implemented 256-QAM modulation algorithms, providing a data rate of 500 kbps in the 433 MHz frequency band [7].

7. The effects of atmospheric turbulence were analyzed. The Cn^2 structural parameter varied between 10^{-14}–10^{-16} $m^{-2/3}$, and attenuation ranged from 0.05 to 0.2 dB/km. Stability was enhanced with wavelengths between 1500–2000 nm [14,16].

8. Quasi-dynamic variations caused 5–15% signal power fluctuations in communication channels. Stability was improved through adaptive optical systems and statistical modeling [21].

9. According to STK simulation results for the 2U cubesat model, the orbital eccentricity was calculated as 86.38°, with a perigee altitude of 434.4 km and an apogee altitude of 450.43 km. The orbital period was determined to be 1.55 hours, and the operational lifetime was estimated at 3.8 years [10].

10. The laser beam control and optical communication systems of the 4U cubesat prototype were successfully tested in the STK environment. The integrated operation of the prototype's subsystems was validated during these tests [15].

RESULTS AND PRACTICAL RECOMMENDATIONS

1. Atayev N.A., Lazer şüalarının idarəedici və aktiv transponder sistemli nano peykin idarəedici alt sistemlərinin nəzəri və alqoritmik tədqiqi // The XXVII International Scientific Symposium "Give way to the Turkic flag!" – Baku: – 2022. – pp. 280-285.
   http://anl.az/down/E.Cavad2022.pdf
2. Həsənov M.H., Atayev N.A., Lazer şüalarının idarəedici və aktiv transponder sistemli nano peykin ilkin konseptual modeli // "Gənclər və elmi innovasiyalar" mövzusunda Respublika elmi-texniki konfrans materialları, AzTU – Bakı: – 2022. – s. 896-902.
   https://www.researchgate.net/publication/366001146_Gnclr_v_elmi_innovasiyalar_movzusunda_Respublika_elmi-texniki_konfrans_materiallari_AzTU
3. Atayev N.A., Study of prototype nanosatellite subsystems based on radio and optical communication technologies // Proceedings Book International Conference on Engineering Sciences (ICES), – Baku: – 2022. - pp. 18-27.
   https://www.iensci.org/library?pgid=l9pslt13-cede6d31-0bb3-48a3-a6f0-ea1952449acf
4. Hasanov M.H., Atayev N.A., Early conceptual model of nanosatellite with laser beam control and active transponder system // IEEE, Systems of Signal Synchronization, Generating and Processing in Telecommunications (SYNCHROINFO), Arkhangelsk: – 2022. – pp.1-4.
   https://doi.org/10.1109/SYNCHROINFO55067.2022.9840919
5. Hasanov M.H., Atayev N.A., Algorithm design nanosatellite based on radio frequency and optical communication // JPIT, Problems of Information Technology, Baku: – 2022. - Vol. 13, No. 2. – pp. 61-68.
   https://jpit.az/uploads/article/en/2022_2/ALGORITHM_DESIGN_OF_NANOSATELLITE_BASED_ON_RADIO_FREQUENCY_AND_OPTICAL_COMMUNICATION.pdf
6. Hasanov M.H., Haciyeva K.H., Atayev N.A., Najafov B.K., Development and Calculation of the Reliability of a 3D Printer //

Springer, Towards Industry 5.0 (ISPR), Lecture Notes in Mechanical Engineering. Cham, Turkey: - 2022, - Vol. 139, No. 5. - pp. 201-210.
https://link.springer.com/chapter/10.1007/978-3-031-24457-5_17

7. Hasanov M.H., Atayev N.A., Conceptual model of a new generation nanosatellite with 3D optical communication switch and radiofrequency transponder // Інформатика, управління та штучний інтелект, – Харків: – 2022. – p. 22.
https://scholar.google.com/citations?user=5tI3A8AAAAAJ&hl=en
8. Atayev N.A., Fostering Space Education in Azerbaijan through Small Satellite Design Program for Undergraduate Students // IAF, 74th International Astronautical Congress (IAC), Baku: - 2023. – pp. 1-13.
https://dl.iafastro.directory/event/IAC-2023/paper/75997/
9. Hasanov M.H., Abdullayev K.I., Piriev S.A., Movsumov A.A., Atayev N.A., FSON Topology for Mass Development and Management of Future Generation Space Technologies // ELSEVIER, Procedia Computer Science, 3rd International Conference on Evolutionary Computing and Mobile Sustainable Networks (ICECMSN), Netherlands: - 2023. - Vol. 230, No. 3. – pp. 82-89.
https://www.sciencedirect.com/science/article/pii/S1877050923020689
10. Atayev N.A., Hasanov M.H., Conceptual design of a communication nanosatellite model with a new generation laser beam control and active transponder system // IAF, Proceedings of the International Astronautical Congress, 74th International Astronautical Congress (IAC), Baku: – 2023. – pp. 1-15.
https://dl.iafastro.directory/event/IAC-2023/paper/76449/
11. Alizade R.İ., Hasanov M.H., Khalilov I.A., Alakbarov A.S., Atayev N.A., Synthesis of New Lunar Parallel Structure Robotic Rowers // IAF, 74th International Astronautical Congress (IAC), Baku: - 2023. – pp. 1-6.
https://dl.iafastro.directory/event/IAC-2023/paper/76434/

12. Atayev N.A., Mutallimov T.A., Mammadov A.T., Reducing deaths in traffic accidents with space research and artificial intelligence // IAF, 74th International Astronautical Congress (IAC), Baku: - 2023. – pp. 1-6.
https://dl.iafastro.directory/event/IAC-2023/paper/80696/
13. Atayev N.A, Hasanov M.H., High-speed data transmission in LEO satellite networks with free space optics-based transponder and 3D switch model // IEEE, 17th International Conference on Application of Information and Communication Technologies, AICT, Baku: – 2023, – pp. 1-6.
https://doi.org/10.1109/AICT59525.2023.10313187
14. Hasanov M.H., Abdullayev K.I., Tagiyev A.D., Gurbanova, G.S., Atayev, N.A., New generation 3D optical switch for free space optical networks // Springer, Intelligent Communication Technologies and Virtual Mobile Networks (ICICV), Lecture Notes on Data Engineering and Communications Technologies, Tirunelveli: – 2023, - Vol. 171, No. 2. – pp.153-162.
https://doi.org/10.1007/978-981-99-1767-9_12
15. Hasanov M.H., Ibrahimov B.Q., Tagiyev A.D., Atayev N.A., Namazov C.B., Najafov, B.K., Investigation of Signal-To-Noise Ratio Based on Optical Compression Systems Using Spectrum in Fso // Jormand Publishing, Advanced Physical Research, Baku: - 2023, - Vol. 5, No. 1. - pp. 33-41.
http://jomardpublishing.com/UploadFiles/Files/journals/APR/V5N1/Hasanov_et_al.pdf
16. Hasanov M.H., Tagiyev A.D., Atayev N.A., Exploration of signal-to-noise ratio with optical compression systems utilizing spectrum in free space optics // 5th International Conference on Problems of Cybernetics and Informatics (PCI), – Baku: – 2023. – pp. 1-3.
https://pci.cyber.az/2023/papers/06.html
17. Atayev N.A., The application directions of SDR technology in a new generation radio communication networks // XXVIII Международная научно-техническая конференция «Современные средства связи», – Минск: – 2023. – p. 50.
r compilation were carried out by the author.

17.pdf

18. Hasanov M.H., Atayev N.A., Conceptual model of a nanosatellite with laser beam transmission and its importance in renewable electrical power harvesting // Energy Sustainability: Risks and Decision Making (ENSUS), Baku: – 2024. - Vol. 2, No. 1. – pp. 1-7.
https://doi.org/10.61413/AEOK4306
19. Hasanov M.H., Piriev S.A., Atayev N.A., Rasullu T.S., Adaptive Monitoring of Free Space Optical Networks Utilizing Artificial Neuron Analysis // IEEE, 3rd International Conference on Applied Artificial Intelligence and Computing (ICAAIC), Salem: - 2024. – pp. 289-292.
https://doi.org/10.1109/ICAAIC60222.2024.10575834
20. Atayev N.A., Bairamov S.N., Actual and future trends of Nanosatellite platforms, ensuring the basic concept level mission design for Sustainable Space // IAF, 75th International Astronautical Congress (IAC), Milan: - 2024. – pp. 1-11.
https://dl.iafastro.directory/event/IAC-2024/paper/81109/
21. Atayev N.A., Hasanov M.H., Integrated Analysis of Atmospheric Performance Models and System-Level Functional Tests for a New Generation Optical Communication Nanosatellite Segment // IAF, 75th International Astronautical Congress (IAC), Milan: - 2024, - pp. 1-13.
https://dl.iafastro.directory/event/IAC-2024/paper/81110/

Author's participation in published works.

[1, 2, 3, 4, 5, 7, 8, 10, 12, 17, 18, 20, 21] – The preparation and compilation of the mentioned works were carried out by the author.

[6, 9, 11, 13, 14, 15, 16, 19] – The investigation of the stated problem, corresponding theoretical calculations, implementation of practical applications, scientific explanations of the results obtained, and their compilation were carried out by the author.

The defense will be held on 14 February 2025 at 14:00 the meeting of the Dissertation council ED 2.41 of the Supreme Attestation Commission under the President of the Republic of Azerbaijan operating at Azerbaijan Technical University.

Address: H.Javid avenue 25, Baku, Azerbaijan, AZ 1073, Azerbaijan Technical University.

Dissertation is accessible at the library of Azerbaijan Technical University.

Electronic versions of dissertation and its abstract are available on the official website of the Azerbaijan Technical University.

Abstract was sent to the required addresses on 13 January 2025.

Signed for print 10.01.2025

Paper format: A5

Volume: 411251

Number of hard copies: 20